

Research Article

A PET/Graphite-Based Triboelectric Nanogenerator for Monitoring the Health of Leg Muscles in Football

Wei Zhang¹ and Xiaoxiang Jiang² 

¹Department of Public Basic Education, Anhui Technical College of Mechanical and Electrical Engineering, Wuhu, Anhui Province 241002, China

²Department of Physical Education, Suzhou University, Suzhou, Anhui Province 234099, China

Correspondence should be addressed to Xiaoxiang Jiang; jiangxiaoxiang@ahszu.edu.cn

Received 15 December 2022; Revised 5 February 2023; Accepted 21 February 2023; Published 5 May 2023

Academic Editor: Kathiravan Srinivasan

Copyright © 2023 Wei Zhang and Xiaoxiang Jiang. This is an open access article distributed under the Creative Commons Attribution License, which permits unrestricted use, distribution, and reproduction in any medium, provided the original work is properly cited.

Recently, self-powered flexible sensors have shown important application value in sports training. Thus, we design a triboelectric nanogenerator based on PET/Graphite composite film (PG-TENG) to harvest human motion energy and monitor football player leg muscle health. The polytetrafluoroethylene (PTFE) film and PET/graphite composite film serve as the triboelectric pairs; meanwhile, the PET/Graphite composite film also plays the role of conductive electrode. Moreover, the PET/graphite composite film can be prepared by a simple reverse molding process. According to the results, the instantaneous power density of PG-TENG can arrive at 5.94 mW/m^2 at $130 \text{ M}\Omega$. The PG-TENG can serve as the motion player to monitor the health of football players' leg muscles and various football sports postures, including the posture of bouncing and dribbling. This research will promote the application of self-driving sensors in sports monitoring.

1. Introduction

In recent years, the large-scale application of Internet of Things (IoT) technology and artificial intelligence technology has encouraged the development of wearable electronic devices [1, 2]. Flexible sensors with tensile properties have potential applications in portable electronic devices, including human posture sensing, medical health monitoring, and sports training [3–5]. It is worth noting that most small wearable devices often need a power supply that can store enough electricity, which limits the service life of wearable electronic devices [6]. Meanwhile, the power supply for portable wearable electronic devices needs to meet the characteristics of low cost, good human compatibility, extensibility, and high strength [7, 8]. Therefore, it is urgent to develop a power generation device that can provide continuous power for wearable electronic devices. Triboelectric nanogenerator (TENG) has been proven to be able to capture the vibration of mechanical energy in the environment and convert it into electrical energy [9–13]. TENG's working principle is based on the triboelectric effect and electrostatic

induction [14, 15]. TENG devices are made of a wide range of materials and can be used to sense various vibrations [16–19]. Among the four working principles of the TENG device, the stretchable TENG device based on the single electrode working principle has the characteristics of simple structure and strong portability [20]. Normally, flexible TENG with tensile function based on single electrode working mode is mainly made of composite conductive materials [21], conductive textiles [21], and hydrogels [22]. Therefore, it is necessary to develop flexible TENG devices with high output performance to meet the power demand of wearable electronic devices.

For hydrogels, because there is a large amount of water inside the gel, it also causes the hydrogel to easily dehydrate due to water evaporation [23]. Hence, a higher dehydration rate will lead to a lower service life of hydrogel, and the mechanical strength will continue to decrease with the evaporation of water. These shortcomings limit the application and development of hydrogel in the TENG field. For conductive fibers, the complex preparation process leads to a high cost, which also leads to their difficult application in

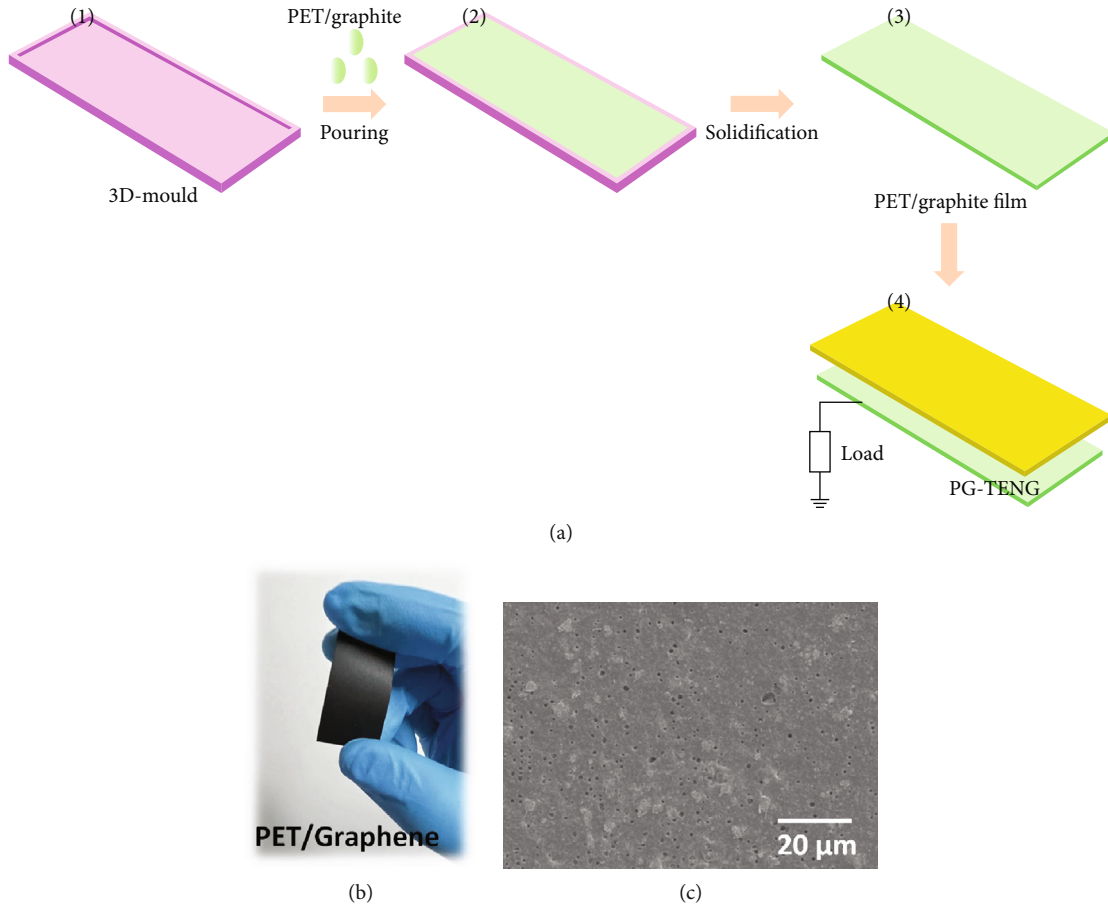


FIGURE 1: (a) (1–3) The preparation process of PET/Graphite film. (a) (4) The structure of PG-TENG. (b) The picture of PET/graphite film. (c) The SEM image of PET/graphite film surface.

TENG devices [24, 25]. Thus, due to their good conductivity and high use strength, the tensile composite conductive materials have a high development potential in the field of preparation of TENG devices. At present, some conductive fillers, such as graphite, metal powder, conductive polymer, and carbon powder, can be incorporated into the elastic matrix as a conductive carriers [26]. Graphite is widely used as electrode material, especially in energy storage electrodes, because of its high conductivity and low cost. In addition, it is also necessary to consider the elastomer as the conductive filler carrier. Generally, the elastomer with high flexibility can be used as the friction material in TENG, and its compatibility with human skin should also be considered. Among many elastomers, PET is widely used in wearable electronic devices due to its nontoxicity, low cost, good human compatibility, and other characteristics.

In this work, we design a triboelectric nanogenerator based on PET/graphite composite film (PG-TENG) to harvest human motion energy and monitor football player leg muscle health. The PG-TENG is based on the single-electrode working mode. The polytetrafluoroethylene (PTFE) film and PET/graphite composite film serve as the triboelectric pairs, meanwhile, the PET/graphite composite film also plays the role of conductive electrode. Moreover, the PET/Graphite composite film can be prepared by a simple reverse molding

process. From the results, the instantaneous power density of PG-TENG can arrive at 5.94 mW/m^2 at $130 \text{ M}\Omega$. It is important that PG-TENG can be used as a human posture sensor to monitor the health of football players' leg muscles and various football sports postures, including the posture of bouncing and dribbling.

2. Experiment

2.1. Fabrication of the PG-TENG. The PG-TENG follows the single-electrode mode. Figure 1(a)-(1) depicts the detailed fabrication process of the PG-TENG device. Firstly, we use 3D printing technology to prepare a concave mold with an internal size of $2 \text{ cm} \times 4 \text{ cm}$, as shown in Figure 1(a)-(1). Then, the graphite powder is doped in the PET solution, and the graphite powder is evenly distributed in the network inside the PET through magnetic stirring. As shown in Figure 1(a)-(2), we pour the PET/Graphite mixed solution into the mold. After 12 h of static curing, the PET/graphite film was successfully prepared, as shown in Figure 1(a)-(3). Finally, PET/graphite film is combined with PTFE film to make the PG-TENG device, as shown in Figure 1(a)-(4). Figure 1(b) illustrates the picture of PET/graphite film, and Figure 1(c) illustrates the SEM image of the PET/graphite film surface.

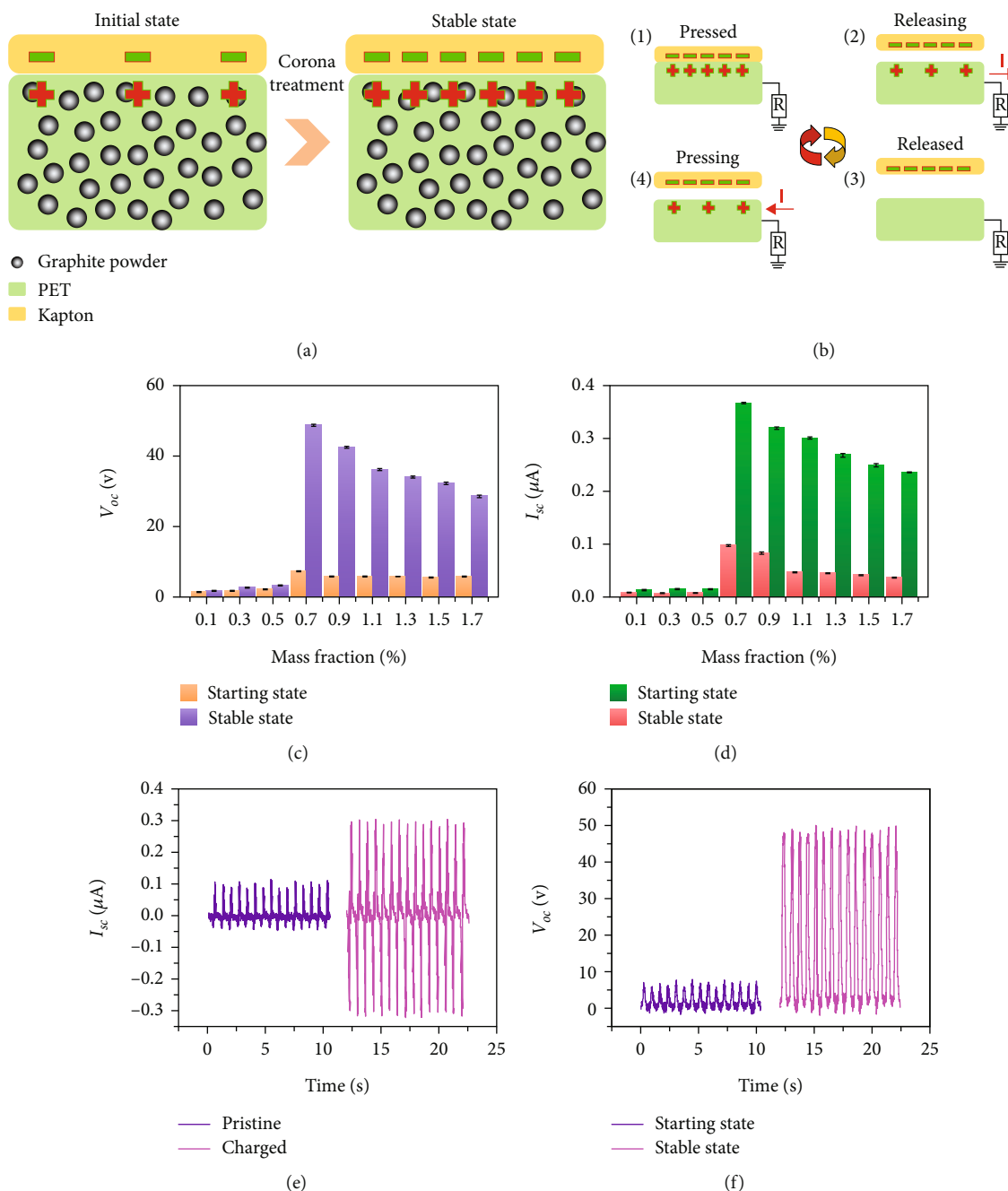


FIGURE 2: (a) Schematic diagram of the triboelectric charges in the surface of Kapton FILM and PET/graphite film after multiple frictions. (b) The working mechanism of PG-TENG. The (c) V_{oc} and (d) I_{sc} of PG-TENG with different mass fractions of graphite. (e, f) Comparison of V_{oc} and I_{sc} of the PG-TENG between starting state and stable state.

3. Results and Discussion

3.1. Working Mechanism of PG-TENG. As depicted in Figures 2(a) and 2(b), the PG-TENG operating mechanism is on the basis of the coupling effect of frictional charging and electrostatic induction. Kapton film functions as a negative triboelectric material, whereas PET/graphite is a positive triboelectric material. Figure 2(a) demonstrates that repeated friction between two kinds of triboelectric materials will lead to the accumulation of a large number of charges

on PET/graphite film, thereby increasing the total amount of triboelectric charges of PET/graphite film. PG-TENG is grounded through wires and operates in single-electrode working mode. Once the surfaces of the two friction materials in PG-TENG are completely in contact, electron transfer will occur at the interface. Since the electric field balance is required for charges with opposite polarity, electrons on the surface of the triboelectric material will not flow into the external circuit. In this design, PTFE film is used as a moving part.

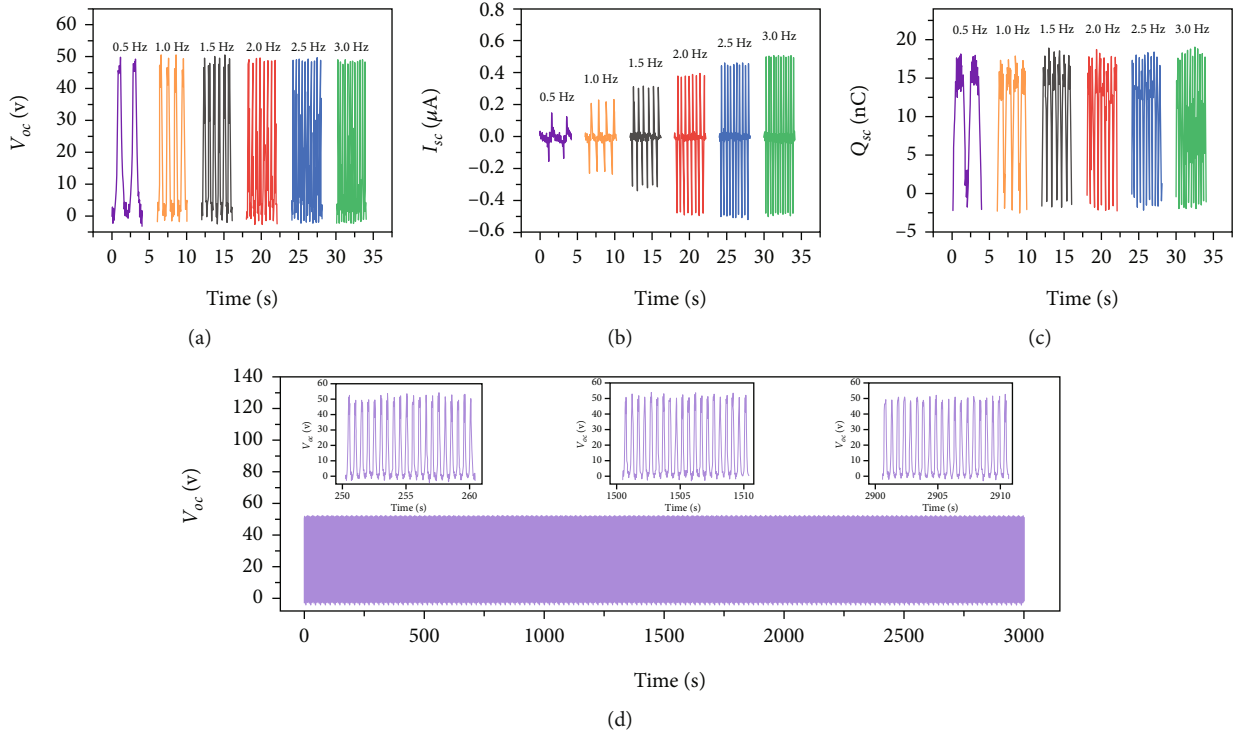


FIGURE 3: (a–c) The V_{oc} , I_{sc} , and Q_{sc} of PG-TENG under different working frequencies from 0.5 Hz to 3.0 Hz. (d) The dependability and stability of PG-TENG.

As shown in Figure 2(b)-(1), under the condition that the surfaces of two triboelectric materials are in full contact, the PET/graphite film surface will generate positive charges and the PTFE film surface will produce negative charges. When the PTFE surface starts to separate from the PET/graphite film surface, the potential difference becomes larger. In order to balance the potential difference, more electrons will flow into PET/Graphite film from the external circuit, as shown in Figure 2(b)-(2). When the separation distance reaches its maximum, there will be no current in the circuit due to the weakening of the electrostatic induction effect, as shown in Figure 2(b)-(3). When the PTFE film is close to the PET/graphite film surface again, electrons will flow from the PET/graphite film surface to the ground, causing a reverse current in the external circuit, as shown in Figure 2(b)-(4).

3.2. Output Performance of PG-TENG. The mechanical motor is used to drive the PTFE film moving parts in a periodic contact separation motion to evaluate the PG-TENG output performance. The contact area of PG-TENG was set at $2 \times 4 \text{ cm}^2$, and the moving distance was 3 cm. To study the influence of the mass fraction of graphite in PET/graphite film on the output performance of PG-TENG, we prepared 9 samples of the same size, and their mass fractions ranged from 0.1% to 1.8%. It is obvious that the output performance of PG-TENG, including V_{oc} and I_{sc} , reaches the highest values at 0.7%, as shown in Figures 2(c) and 2(d). For the two states where the triboelectric charge saturation has not been reached and the triboelectric charge saturation has been reached, the output performance continues to

decline with the increase of the mass fraction of graphite. The reason for this result is that when the content of Graphite is low, the charge storage effect of PET/graphite is poor, and when the content of graphite increases, the triboelectric charge generation of graphite will be affected, so there is an optimal value of the mass fraction. As shown in Figures 2(e) and 2(f), the PG-TENG with 0.7% graphite can bring a V_{oc} of 49.2 V and an I_{sc} of $0.3144 \mu A$, respectively.

In a general sense, one of the factors that has an effect on the amount of electrical output that TENGs produce is the operating frequency. To delve deeper into the topic of frequency dependence, the previous standards of PG-TENG with 0.7% graphite were also assessed at different frequencies. From 0.5 to 3.0 Hz, there is no substantial change in the output of V_{oc} and Q_{sc} , and the maxima at 49.2 V and 16.8 nC, respectively, remain virtually unchanged, as shown in Figures 3(a) and 3(c). According to the results, the V_{oc} and Q_{sc} of PG-TENG are independent of the operating frequency. Figure 3(b) demonstrates that when the working frequency increases, the I_{sc} rises from $0.15 \mu A$ to $0.5 \mu A$. This phenomenon is caused by the rise in the velocity of the movable friction layer as the operating frequency increases at a given distance, which ultimately results in a greater electron transfer rate and a higher current output. Besides, the dependability and stability of the PG-TENG device are crucial evaluation considerations. Consequently, it is crucial to explore the properties mentioned above of PG-TENGs. Figure 3(d) demonstrates that the V_{oc} of PG-TENG remains stable even after 5000 cycles of contact separation up to 3000 s, showing that PG-TENG is highly reliable and stable.

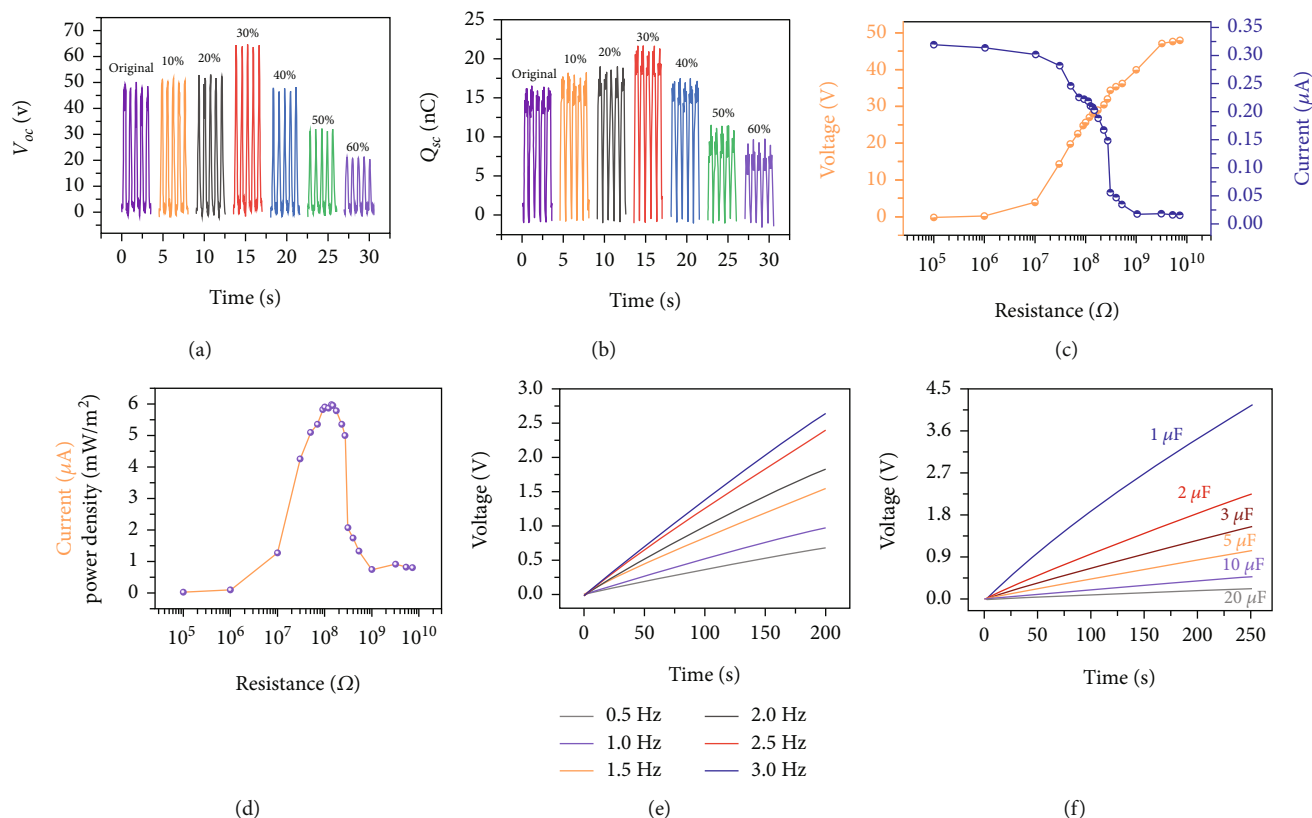


FIGURE 4: (a, b) The electrical output of PG-TENG under different tensile amplitudes. (c, d) The output voltage, output current, and output power density of PG-TENG under different resistance. (e) The charging curves of PG-TENG for a $2 \mu\text{F}$ capacitor under different working frequencies. (f) The charging curves of PG-TENG for different capacitors under the frequency of 2 Hz.

The deformability under varying tensile strains and the related electrical output are critical requirements for a wide variety of applications for stretchable single-electrode TENGs. Additional research was conducted on the mechanical properties of PG-TENGs and the accompanying evaluation tests, including electrical output. Owing to the remarkable stretchability of PET/graphite film, the electrical output of PG-TENG under a variety of strains was also investigated. For the purpose of this test, the original size was scaled back to 70% of the strain because the strain caused by the skin surface and joint motion does not surpass this threshold. At various levels of tensile strain, including V_{oc} and Q_{sc} , the electrical output of PG-TENG increased until 30% strain (V_{oc} : 64.8 V and Q_{sc} : 20.4 nC) and subsequently fell dramatically, as shown in Figures 4(a) and 4(b). We can attribute this result to the coupling effect of the lower conductivity of PET/Graphite film and the larger contact area. When PG-TENG is stretched, the conductivity of the conductive network composed of graphite drops gradually due to the gradual reduction of the overlap area and the loss of conductive routes. In the beginning, only a portion of the network is stretched. Both the passage of electrons and the generation of electricity are maintained by the conductive channels. During this interim period, the contact surface area will first increase as the PG-TENGs are extended before beginning to decrease. Stretching the PG-TENG further destabilizes the conductive network, resulting in a shorter

conductive channel. As a result, fewer electrons may travel through the gadget, and the electrical output decreases further. Therefore, the favorable impacts of sustained electrical conductivity and contact area can be attributed to the early stages of elongation of electrical output performance from the initial state to 30% distortion. This can be said to have occurred when the electrical output performance was extended from the original state. Further stretching to 60% diminishes electrical output performance due to the negative impacts of decreased conductivity and decreased contact area.

The PG-TENG has a good power generation function, thus, it has great potential to use PG-TENG as a potential energy harvester. The formula $P = U^2/(RS)$, where U is the output voltage, R is the load resistance and S is the effective area of the PG-TENG, can be used to compute the effective power density (P) of a PG-TENG. As illustrated in Figure 4(c), the output voltage of PG-TENG grows with the increase of external load resistance, while the current decreases according to Ohm's law. As a direct consequence of this, the instantaneous power density of PG-TENG rises until it reaches a maximum of roughly 5.94 mW/m^2 at $130 \text{ M}\Omega$ and then continues to decrease, as shown in Figure 4(d). The charging rate gradually increases as the frequency increases, as presented in Figure 4(e). Also, the charging capabilities of PG-TENG for various capacitors are also investigated, as shown in Figure 4(f). In detail, a

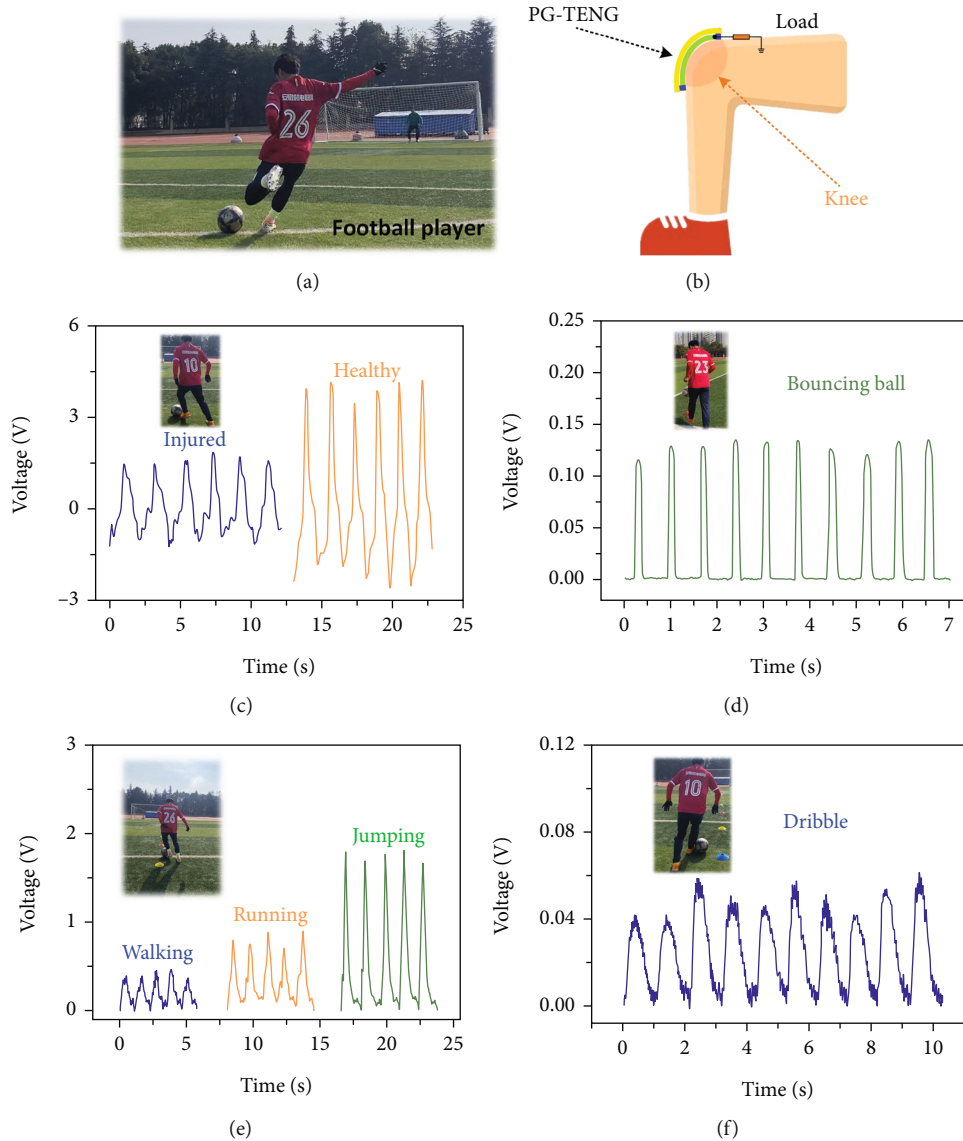


FIGURE 5: (a) The photograph of a football player. (b) The structure diagram of PG-TENG installed on the human knee. (c) The output voltage signal of PG-TENG by mimicking injury and health. (d) The output voltage signal of PG-TENG in bouncing ball motion. (e) The output voltage signal of PG-TENG under walking, running, and jumping. (f) The output voltage signal of PG-TENG under dribble motion.

$1 \mu\text{F}$ capacitor could be charged to 4.2 V in 250 s. In contrast, a $2.2 \mu\text{F}$ capacitor can be charged to 2.25 V in 193 s, illustrating that the charging rate increases steadily with decreasing capacity.

As we all know, football is a game that requires players to complete some short-time maximum and close to the maximum physical capacity limit actions, such as sprinting, jumping, and changing direction, to fight with opponents to win the ball. To improve the explosive power of football players' lower limbs, relevant muscle training programs are widely used in football. These training methods will induce neuromuscular adaptability and coordination within and between muscles, thus improving the comprehensive ability of football players. In this work, we use the PG-TENG device as a self-powered motion sensor to monitor the lower limb muscle health during soccer operation, as shown

in Figure 5(a). As we all know, athletes will suffer from lower limb muscle injuries during long-term training, which will be fed back through lower limb movement posture. Therefore, the lower limb muscle health can be monitored by monitoring the lower limb movement posture. In detail, we put PG-TENG in the knee position of the leg, as shown in Figure 2(b). When the lower limb moves, PG-TENG installed at the knee will produce slight vibration, which will make it generate a voltage signal to reflect the player's posture. As shown in Figure 5(a), we compared the output signals generated by PG-TENG under injury and health conditions by imitating leg movements under injury conditions. It can be clearly found that when the leg muscles are injured, the lower limb movement will be limited, which can be reflected by the sensing signal. Furthermore, it can also record the training information of

the players in the bouncing ball training, as shown in Figure 5(d). Moreover, when players walk, run, and jump, PG-TENG can still produce output voltage signals with different signal characteristics, as shown in Figure 5(e). PG-TENG can also be used to monitor the motion information in the dribble motion, as shown in Figure 5(f). Obviously, the athlete is able to tell the injury as soon as it happens when the muscle is injured and the motion is limited. However, when the human injury is in the recovery period, the movement of the injured part will be limited, but the limited extent is difficult for doctors to accurately evaluate through the patient's description. Through the designed PG-TENG sensor, the rehabilitation process can be quantitatively evaluated and the basis for postinjury rehabilitation treatment can be provided. Thus, the PG-TENG can monitor the muscle health of football players and the information during football training.

4. Conclusion

In summary, we design a PG-TENG to harvest human motion energy and monitor football player leg muscle health. The triboelectric pairs consist of polytetrafluoroethylene (PTFE) film and PET/graphite composite film, and PET/graphite composite film also plays the role of conductive electrode. The PG-TENG has good tensile properties. Under different tensile conditions, the output properties of PG-TENG are studied. Moreover, the PET/Graphite composite film can be prepared by a simple reverse molding process. According to the results, the instantaneous power density of PG-TENG can arrive at 5.94 mW/m^2 at $130 \text{ M}\Omega$. Moreover, the PG-TENG can serve as the motion player to monitor the health of football players' leg muscles and various football sports postures, including the posture of bouncing and dribbling.

Data Availability

All data generated or analyzed during this study are included in this published article.

Conflicts of Interest

The authors declare that they have no conflicts of interest.

References

- [1] M. Abdullahi, Y. Baashar, H. Alhussian et al., "Detecting cybersecurity attacks in internet of things using artificial intelligence methods: a systematic literature review," *Electronics*, vol. 11, no. 2, p. 198, 2022.
- [2] X. Cao, Y. Xiong, J. Sun, X. Zhu, Q. Sun, and Z. L. Wang, "Piezoelectric nanogenerators derived self-powered sensors for multifunctional applications and artificial intelligence," *Advanced Functional Materials*, vol. 31, no. 33, article 2102983, 2021.
- [3] Z. Lu, Y. Zhu, C. Jia et al., "A self-powered portable flexible sensor of monitoring speed skating techniques," *Biosensors*, vol. 11, no. 4, p. 108, 2021.
- [4] K. Guo, S. Zhang, S. Zhao, and H. Yang, "Design and manufacture of data gloves for rehabilitation training and gesture recognition based on flexible sensors," *Journal of Healthcare Engineering*, vol. 2021, Article ID 6359403, 9 pages, 2021.
- [5] X. Ye, B. Shi, M. Li et al., "All-textile sensors for boxing punch force and velocity detection," *Nano Energy*, vol. 97, article 107114, 2022.
- [6] C. Ma, M. G. Ma, C. Si, X. X. Ji, and P. Wan, "Flexible MXene-based composites for wearable devices," *Advanced Functional Materials*, vol. 31, no. 22, article 2009524, 2021.
- [7] Y. Cheng, K. Wang, H. Xu, T. Li, Q. Jin, and D. Cui, "Recent developments in sensors for wearable device applications," *Analytical and Bioanalytical Chemistry*, vol. 413, no. 24, pp. 6037–6057, 2021.
- [8] H. C. Ates, A. K. Yetisen, F. Güder, and C. Dincer, "Wearable devices for the detection of COVID-19," *Nature Electronics*, vol. 4, no. 1, pp. 13–14, 2021.
- [9] Y. Kim, D. Lee, J. Seong, B. Bak, U. H. Choi, and J. Kim, "Ionic liquid-based molecular design for transparent, flexible, and fire-retardant triboelectric nanogenerator (TENG) for wearable energy solutions," *Nano Energy*, vol. 84, article 105925, 2021.
- [10] W. He, X. Fu, D. Zhang et al., "Recent progress of flexible/wearable self-charging power units based on triboelectric nanogenerators," *Nano Energy*, vol. 84, article 105880, 2021.
- [11] H. Zhao, R. Su, L. Teng et al., "Recent advances in flexible and wearable sensors for monitoring chemical molecules," *Nanoscale*, vol. 14, no. 5, pp. 1653–1669, 2022.
- [12] W. Li, L. Lu, A. G. P. Kottapalli, and Y. Pei, "Bioinspired sweat-resistant wearable triboelectric nanogenerator for movement monitoring during exercise," *Nano Energy*, vol. 95, article 107018, 2022.
- [13] N. Zheng, J. Xue, Y. Jie, X. Cao, and Z. L. Wang, "Wearable and humidity-resistant biomaterials-based triboelectric nanogenerator for high entropy energy harvesting and self-powered sensing," *Nano Research*, vol. 15, no. 7, pp. 6213–6219, 2022.
- [14] N. Sun, G. G. Wang, H. X. Zhao et al., "Waterproof, breathable and washable triboelectric nanogenerator based on electrospun nanofiber films for wearable electronics," *Nano Energy*, vol. 90, article 106639, 2021.
- [15] H. Zhang, P. Zhang, L. Deng et al., "Three-dimensional polypyrrole nanoarrays for wearable triboelectric Nanogenerators," *ACS Applied Nano Materials*, vol. 5, no. 8, pp. 11219–11228, 2022.
- [16] D. Bhatia, S. H. Jo, Y. Ryu, Y. Kim, D. H. Kim, and H. S. Park, "Wearable triboelectric nanogenerator based exercise system for upper limb rehabilitation post neurological injuries," *Nano Energy*, vol. 80, article 105508, 2021.
- [17] J. Jeong, S. Jeon, X. Ma, Y. W. Kwon, D. M. Shin, and S. W. Hong, "A sustainable and flexible microbrush-faced triboelectric generator for portable/wearable applications," *Advanced Materials*, vol. 33, no. 39, article 2102530, 2021.
- [18] H. Shen, H. Lei, M. Gu et al., "A wearable electrowetting on dielectrics sensor for real-time human sweat monitor by triboelectric field regulation," *Advanced Functional Materials*, vol. 32, no. 34, article 2204525, 2022.
- [19] J. Gu and K. Ruan, "Breaking through bottlenecks for thermally conductive polymer composites: a perspective for intrinsic thermal conductivity, interfacial thermal resistance and theoretics," *Nano-Micro Letters*, vol. 13, no. 1, 2021.

- [20] W. Yuan, C. Zhang, B. Zhang et al., "Wearable, breathable and waterproof triboelectric nanogenerators for harvesting human motion and raindrop energy," *Advanced Materials Technologies*, vol. 7, no. 6, article 2101139, 2022.
- [21] Y. Yang, B. Xu, Y. Gao, and M. Li, "Conductive composite fiber with customizable functionalities for energy harvesting and electronic textiles," *ACS Applied Materials & Interfaces*, vol. 13, no. 42, pp. 49927–49935, 2021.
- [22] X. Luo, L. Zhu, Y. C. Wang, J. Li, J. Nie, and Z. L. Wang, "A flexible multifunctional triboelectric nanogenerator based on MXene/PVA hydrogel," *Advanced Functional Materials*, vol. 31, no. 38, article 2104928, 2021.
- [23] F. G. Torres, O. P. Troncoso, and G. E. De-la-Torre, "Hydrogel-based triboelectric nanogenerators: properties, performance, and applications," *International Journal of Energy Research*, vol. 46, no. 5, pp. 5603–5624, 2022.
- [24] M. Chen, Z. Wang, Q. Zhang et al., "Self-powered multifunctional sensing based on super-elastic fibers by soluble-core thermal drawing," *Nature Communications*, vol. 12, no. 1, pp. 1–10, 2021.
- [25] C. Fan, Y. Zhang, S. Liao, M. Zhao, P. Lv, and Q. Wei, "Manufacturing technics for fabric/fiber-based triboelectric nanogenerators: from yarns to micro-nanofibers," *Nanomaterials*, vol. 12, no. 15, p. 2703, 2022.
- [26] S. Sharma, P. Sudhakara, A. A. B. Omran, J. Singh, and R. A. Ilyas, "Recent trends and developments in conducting polymer nanocomposites for multifunctional applications," *Polymers*, vol. 13, no. 17, p. 2898, 2021.